RESEARCH ARTICLE

Inhibitors of EYA3 Protein in Ewing Sarcoma

Fahad Hassan Shah, Song Ja Kim*

Abstract

Objective: Among sarcomas, Ewing sarcoma (EWS) is characterized as a highly malignant type of bone tumor caused by the fusion of EWS RNA Binding Protein-1 (EWSR1)/ Friend leukemia integration 1 (FLI1) genes. The product of fusion gene gives rise to EWSR1/FLI1 which activates the activity of Eyes absent homolog 3 (EYA3) which causes tumor growth and angiogenesis. EYA3 is now considered as a therapeutic drug target for EWS . The study was designed to gather potential inhibitors for the EYA3 target using medicinal compounds. **Methods:** In this study, we have obtained a list of medicinal compounds from the NuBBE database and downloaded their structural information. Then insilico screening analysis of >2,000 medicinal compounds was performed with PyRX virtual drug screening software to discover potential inhibitors for the treatment of EWS. **Results:** Our investigation revealed that Sorbifolin and 1,7-Dihydroxy-3-methylanthracene-9.10-dione show interactive affinity for EYA3 active residues. Moreover, these compounds have adequate toxicity, can induce cytotoxicity in EWS cells, and are capable of regulating the expression of genes activated by EWSR1/FLI1. **Conclusion:** Our study concluded that Sorbifolin and 1,7-Dihydroxy-3-methylanthracene-9.10-dione are promising drug candidates for the treatment of EWS and should be further subjected to invitro testing.

Keywords: Eyes Absent Homolog-3- Ewing Sarcoma- Virtual Screening- Medicinal Compounds- In silico Gene

Introduction

The Ewing sarcoma (EWS) is an aggressive and metastasis prone bone tumor which commonly affects the younger adolescents and children. After osteosarcoma, it is the second frequently reported bone tumor affecting the age group of <15 years (Bellan et al., 2015; Lupo et al., 2021). Epidemiological studies show that almost 3 children per million are affected from this disease in the United States (Campbell et al., 2018; Kabir et al., 2021). Patients with this disease have a survival rate of 70-80 %, whereas some cases result in metastasis which substantially reduces the survival rate to 30 % (Grünewald et al., 2018). Treatments for these tumors are comprised of radiotherapy, chemotherapy, and surgery. However, a rise in atypical morphological and cellular changes, and the elusive molecular nature of Ewing sarcoma are making these tumors more resistant to treatment and are more susceptible to metastasis and aggressive recurrence (May et al., 2013; Ahmed et al., 2014). In this disease, chromosomal translocation between chromosomes 11 and 22 causes the fusion of Ewing's sarcoma breakpoint region 1 (EWSR1) to the Friends leukemia virus integration 1 (FLI1) (Kabir et al., 2021). This integration encodes for the EWS-FL1 fusion protein, allowing the manipulation of gene expression in order to instigate uninterrupted cell division, and onco- and angio- genesis, leading to tumor formation. Efforts have been made to design EWS-FL1

inhibitors which stunt the rapid proliferation of tumor cells. Candidates such as PARP, LSD1, and insulin growth factor-1 receptor inhibitors have been tested in the clinical trials. However, these drugs failed to show any discerning activity against this disease, and therefore, there are calls for further molecular exploration into new protein targets.

EYA3 belongs to the family of eyes absent protein. This protein plays a vital role during embryogenic development, and afterwards its activity is silenced after development. Recently, Wang and colleagues studied the molecular mechanism of Ewing sarcoma in the A673 cell line (Wang et al., 2021). They have identified the upregulation of EYA3 by EWS-FLI fusion protein, expediting cell division and tumor growth. This upregulation of EYA3 also in turn activates the expression of other proteins which are involved in cell growth, apoptosis, survival, angiogenesis, invasion, and migration. Inhibiting the activity of EYA3 stunts the growth of Ewing cells and the metastatic potential and could be the next promising therapeutic target for drug discovery and development studies.

In this article, we unraveled the hidden potential of thousands of medicinal compounds with a good pharmacokinetic and toxicity profile against EYA3 protein, using a virtual screening method. The screened compounds were further analyzed to record the effects on gene targets and A673 lines, using in silico prediction databases.

Department of Biological Sciences, College of Natural Sciences, Kongju National University, Gongju 32588, Republic of Korea.
*For Correspondence: ksj85@kongju.ac.kr

Materials and Methods

Construction and Validation of Protein Model

The Eyes absent homolog 3 (EYA3) protein was designed with Swiss-model (Kopp et al., 2004) by retrieving the protein sequence (Sequence ID: CAA7131) from the NCBI protein. The Swiss-model database built the 3D-structure of the EYA3 protein, which was then refined and minimized with GalaxyRefine database (Heo et al., 2013). After refinement, the structural and topological features of the EYA3 protein template was determined using protein model validation database such as ERRAT, Verify 3D, ProCHECK, Pro-SA, VADAR and ResPROX (Shah et al., 2021).

Prediction of Active Site Residues

The 3D-generated protein model was then further used to predict the ligand binding residues in order to determine the chemical affinity of medicinal ligands. Active site residues within the EYA3 protein were predicted by Prank-Web (Jendele et al., 2019). The refined and validated structure of the EYA3 protein was then uploaded onto the Prank-Web database; this predicted the active pockets based on ranks, pocket score, probability score, and conservation analysis. We selected pocket 1 based on high scores across these categories.

Virtual Screening Setup

Molecular docking of >2,000 medicinal ligands obtained from NuBBE (Pilon et al., 2017) against the EYA3 protein was performed with PYRX 0.8 software, which evaluates the interaction between ligands and receptor. The active site residues predicted by Prank-Web (Jendele et al., 2019) was specified to allow site specific interaction of ligands. The results obtained from the virtual screening analysis was further refined based on hydrogen bonding of ligands with the receptor's defined active residues, binding energy, and inhibitory constant. The structural stability of docked models was then compared to the reference ligand (Benzarone: PubChem ID: 255968), in order to predict the stability of the docked ligand. This was achieved using the LigRMSD database (Velázquez-Libera et al., 2020).

Toxic Dose, Adverse Effects and Specific Organ Damage Prediction

The GUSAR (Lagunin et al., 2011), Adver-Pred (Ivanov et al., 2018), and ROSC-Pred databases (Lagunin et al., 2018) were used to investigate the acute toxicity, compounds side effects and damaging effects of successful

ligands. The canonical SMILES of ligands were exploited to predict these elements.

PASS Analysis, Gene Expression and Cell Lining Studies

The PASS online (Poroikov et al., 2003), DIGEP-Pred (Lagunin et al., 2013) and PaccMann databases (Cadow et al., 2020) were used to document the effects of ligands on biological, molecular, and genetic activity of this disease.

Results

Model Construction and Validation

A homology modelling method was applied to construct the structure of EYA3, using the sequence acquired from the NCBI Protein database. The structure of EYA3 was not found in the RCSB Protein database, necessitating the manual construction of the protein model using the Swiss-model. This database constructed the EYA3 model by using 4EGC.1. B (Human EYA2 Eya domain) as a template. Because the EYA3 sequence shows 66.78 % sequence similarity with Eyes absent homolog 2: The global model quality estimate value was 0.31 and QMEAN was 0.25.

The generated model had low QMEAN score and potential structural irregularities, both of which required refinement and minimization. This was achieved through GalaxyRefine database, which further improved the structural and topical features of EYA3 protein model. The 3D model was then validated with ERRAT, Verify3D, and ProCHECK: the generated model had a quality factor of 99.2%, with more than 80 % of amino acids scoring 0.2 in the 3D/1D profile which qualified Verify3D criteria (Table 1). The stereochemical features of this model showed that 95.8 % of amino acids were in favorable region and 3.8 % were in additionally allowed region, whereas single residue SER438 was in disallowed region in the Ramachandran plot. Pro-SA results indicated that the 3D model of EYA3 had a Z-score of -8.95. The negative value indicate that the generated protein structure possesses no errors, aberrant energy fluctuations, or structural abnormalities. There are 146 helices, 29 beta sheets, 96 coils and 56 turns in the structure of EYA3 as evaluated by VADAR. The predicted resolution of EYA3 model is 1.565 Å, which is considered good and valid for a constructed protein structure as proven by ResProX.

Active Site Residues in EYA3

The active site residues were identified in order to direct the medicinal ligands toward the active pocket and inhibit the protein activity of EYA3. PrankWeb results

Table 1. The Structural Assessment of Constructed 3D Protein Model of EYA3.

| Protein Model	Ramachandran Plot Results	ERRAT Score	VERIFY 3D Results	Pro-SA Results	ResPROX Protein Resolution	VADAR Results
EYA3	Residues in Favorable Region: 230 (95 %) Residues in Additionally Allowed region: 9 (3.8 %) Residues in Disallowed Region: 1 (0.4 %)	99.216	99.26% of the residues have averaged 3D-1D score (0.2) PASSED	-8.95	1.565 Å	Helix: 146 (53 %), Beta: 29 (10%), Coil: 96 (35%), Turn: 56 (20%)
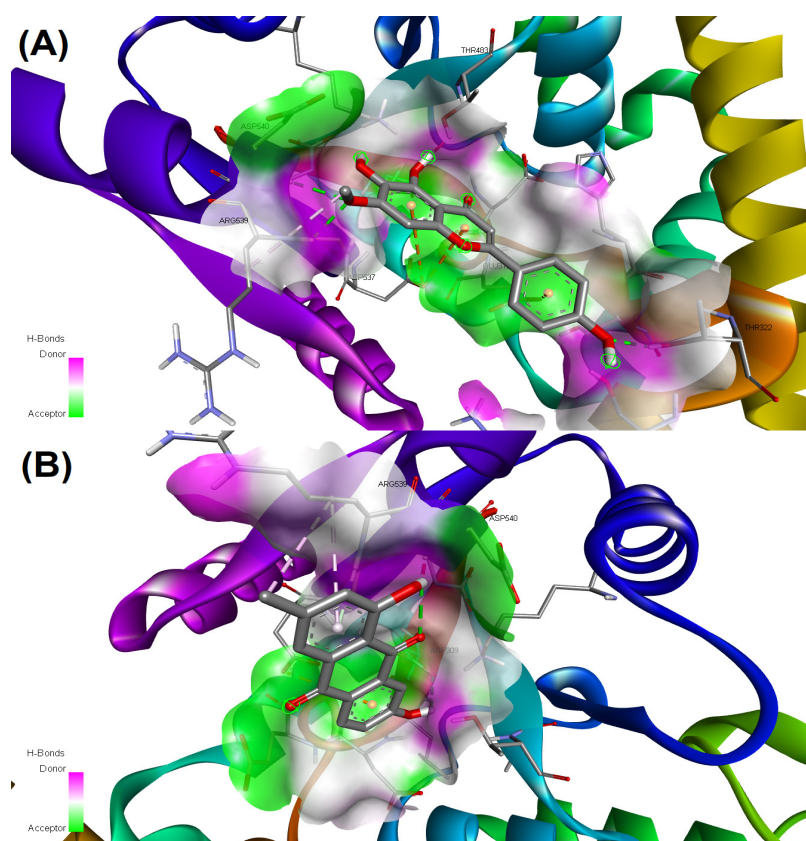
Figure 1. Interaction of Medicinal Compounds with EYA3 Protein Target. (A) Sorbifolin, (B) 1,7-Dihydroxy-3-methylanthracene-9.10-dione.

indicated that Pocket RANK 1 had a pocket score of 8.19, and a probability score of 0.129. The active amino acids surrounding the active pocket of EYA3 was 10 and the recorded conservation score was 0.675. The predicted active amino acids are ASP309, ASP311, GLU312, HIS318, THR483, LYS515, ASP537, GLY538, ARG539, and ASP540. The residues were then further used to determine the interaction of medicinal ligands with these amino acids of the EYA3 protein.

Virtual Screening Results

The interaction analysis showed that two natural compounds Sorbifolin and 1,7-Dihydroxy-3-methylanthracene-9.10-dione made hydrogen bonds with the active amino acids of EYA3 (Table 2) (Figure 1). Sorbifolin used terminal hydroxyl groups to form hydrogen bonds with THR322, ARG539 and ASP540, whereas benzene rings participated in the formation of pi-anion interaction with GLY312, and ASP537 (Figure 2 A). Similarly, 1,7-Dihydroxy-3-methylanthracene-9.10-dione

Table 2. Profile of Docking Interaction of Ligands with EYA3 Receptor

Ligands	Intermolecular Energy	Inhibition Constant	Prank-Web Predicted Residues	Hydrogen Interaction of ligands with Residues	LigRMSD Values (Reference Ligand: Benzarone)
Sorbifolin	-5.8 kcal/mol	119.59μM	ASP309. ASP311, GLU312, HIS318, THR483, LYS515, ASP537, GLY538. ARG539, ASP540	THR322, ARG539, ASP540	2.63Å
1,7-Dihydroxy-3-methylanthracene-9.10-dione	-5.9 kcal/mol	71.80μM		ASP309	2.24Å

Table 3. Nature of Toxicity of Screened Medicinal Ligands

| Ligands	Side Effects	Organ Specific Damage	Intravenous Route Toxicity Value	Oral Route Toxicity Value	Subcutaneous Route Toxicity Value	Intraperitoneal Route Toxicity Value
Sorbifolin	Hepatotoxicity	urinary bladder, kidney, and stomach	1,552,000 mg/kg	1907,000 mg/kg	3784,000 mg/kg	644,400 mg/kg
1,7-dihydroxy-3-methylanthracene-9.10-dione	cardiac failure and hepatotoxicity	urinary bladder, kidney, stomach, and pituitary gland	120,000 mg/kg	436,700 mg/kg	887,600 mg/kg	1602,000 mg/kg
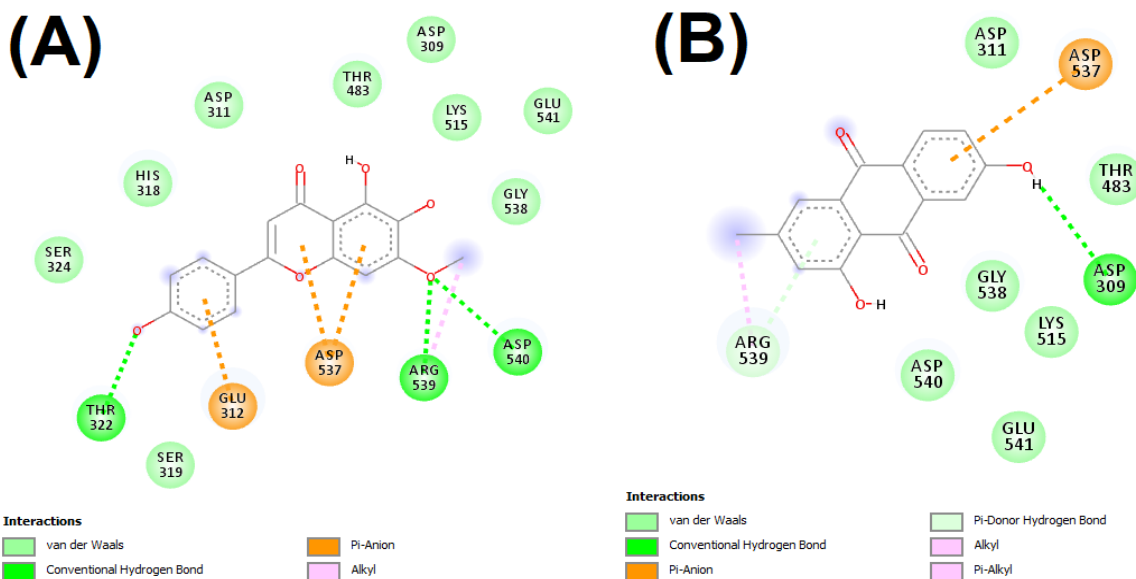
Figure 2. Chemical Interaction of Medicinal Compounds with Active Amino acid subunits of EYA3 Protein Target. (A) Sorbifolin, (B) 1,7-Dihydroxy-3-methylanthracene-9.10-dione.

Table 4. Prediction of Spectra of Activity of Screened Medicinal Ligands

Ligands	Pa	Biological Activity
Sorbifolin	0.932	HIF1A expression inhibitor
	0.905	TP53 expression enhancer
	0.798	Antineoplastic
1,7-Dihydroxy-3-methylanthracene-9, 10-dione	0.795	HIF1A expression inhibitor
	0.772	TP53 expression enhancer
	0.75	Antineoplastic

Figure 3. Structural Regions of (A) Sorbifolin and (B) 1,7-Dihydroxy-3-methylanthracene-9. 10-dione involved in inducing cytotoxicity in A673 Cells.

also utilized hydroxyl group to make hydrogen bond with ASP309 and the benzene ring established pi-anion interaction with ASP537 (Figure 2 B). The intermolecular binding energy between ligands and the receptor was -5.8 and -5.9 kcal/mol, whereas inhibitory constant values were 119.59 and 71.80 µM, respectively. The docked structures of these two ligands were then compared with benzarone to predict the RMSD value using LigRMSD. Results showed that 1,7-dihydroxy-3-methylanthracene-9.10-dione had the RMSD of 2.24 Å, and 2.63 Å for Sorbifolin, which are adequately stable values (Shah et al., 2020, 2021).
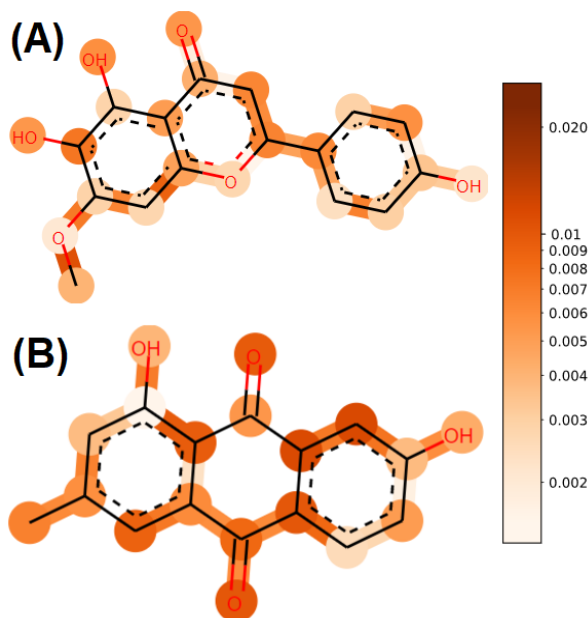
Table 5. Gene Expression Pattern Induced by Screened Medicinal Ligands

Ligands	Gene Expression Pattern	% Age Inhibition or Modulation	Function of Gene in Ewing's Sarcoma	Reference
Sorbifolin	E2F5 ↓	81.7% Suppression	Increases Tumor cell division	(Schwentner et al., 2015)
	STEAP1 ↓	75.2% Suppression	Stimulate Invasive phenotypes formations	(Grunewald et al., 2012)
	NOTCH1 ↑	82.4% Modulation	Downregulation of NOTCH1 pathway reduces tumor cell apoptosis	(Di Muccio et al., 2005)
1,7-dihydroxy-3-methylanthracene-9.10-dione	CTSD ↓	94.4% Suppression	Promotes Cell metastasis	(Gemoll et al., 2015)

Table 6. Effect of Screened Compounds on A673 Cell Line of Ewing Sarcoma

Ligands	Histology	Site	Cell Line	IC$_{50}$ Log (μmol)
Sorbifolin	Ewing's sarcoma peripheral primitive neuroectodermal tumor	Soft tissue	A673	2.48371 2.48131
1,7-dihydroxy-3-methylanthracene-9.10-dione		Bone		1.78391

Toxicity Profile Results

Toxicity profiling was performed to predict the lethal dose, degree of safety, and therapeutic index of a compound in a rodent model. Sorbifolin has the following lethal dose values: 1,907,000 mg/kg, for the oral route, 1,552,000 for the intravenous route, 3,784,000 mg/kg for the subcutaneous and 644,400 mg/kg for the intraperitoneal route, and is a class 5 chemical (Table 3). Whereas 1,7-Dihydroxy-3-methylanthracene-9.10-dione, the values are:1,602,000 mg/kg for intraperitoneal route, 436,700 mg/kg for the oral route, 120,000 mg/kg for the intravenous route and 887,600 mg/kg for the subcutaneous route and is a class 4 chemical. An overdose of both Sorbifolin and 1,7-Dihydroxy-3-methylanthracene-9.10-dione can cause hepatoxicity. In case of 1,7-Dihydroxy-3-methylanthracene-9.10-dione, it can also cause cardiac failure. The toxic effects of 1,7-dihydroxy-3-methylanthracene-9.10-dione can harm the urinary bladder, kidney, stomach, and pituitary gland whereas Sorbifolin affects the urinary bladder, kidney, and stomach only.

Prediction of Activity Spectra for Substances (PASS) Analysis

The biological activity of these compounds was determined across 3000 pharmacologically active targets in order to elucidate the molecular mechanism of action. Both compounds are HIF1-alpha expression inhibitors which prevents the proliferation of tumor cells inducing apoptosis (El-Naggar et al., 2015). They upregulate the activity of TP53, which increases the tumor suppressor activity (Thoenen et al., 2019). They are are anti-neoplastic agents (Table 4).

Gene Expression Studies

Gene expression studies revealed some promising results that can further aid in the prevention of Ewing sarcoma's aggressive growth (Table 5). It was observed that Sorbifolin downregulates the activity of E2F5, which is uninterruptedly increased in this disease, allowing continuous cell division. This leads to the formation and expansion of tumors (Schwentner et al., 2015). It also decreases the expression of STEAP1, which is involved in the formation of invasive phenotypes and cell metastasis (Grunewald et al., 2012). Sorbifolin can help to stimulate NOTCH1, by inducing apoptosis in tumor cells (Di Muccio et al., 2005). In case of 1,7-dihydroxy-3-methylanthracene-9.10-dione downregulated CTSD gene expression (Gemoll et al., 2015), This makes cells less vulnerable to metastasis.

Cell Lining Studies

According to Wang et al., (2021), inhibited the EYA3 protein target in A673 EWS cell line and RD-ES cells. We took the similar approach, by using A673 in the PaccMann database to evaluate the cytotoxic effects of these compounds (Table 6). Sorbifolin induced cytotoxicity in A673 cells, using hydroxyl and oxy groups along with carbon of its benzene rings: the IC50 value recorded was 2.48 log(μmol) whereas 1,7-dihydroxy-3-methylanthracene-9.10-dione also induced cytotoxicity by using oxy groups and carbons of anthracene. The IC50 value recorded was 1.78 log(μmol) for soft tissue and 1.73 log(μmol) for bone tumor (Figure 3).

Discussion

The progression of a continuous cell cycle and DNA damage repair mechanism is highly upregulated in Ewing sarcoma tumors. This is due to the activity of the EYA3 protein which encourages tumor growth and angiogenesis (Wang et al., 2021). EWS-FLI is the master regulatory and faulty fusion protein which promotes the oncogenesis in EWS cells and upregulates the activity of EYA3 by inhibiting miRNA-708 (Robin et al., 2012). The main function of miRNA-708 is to switch off cell proliferation activity after embryonic development (Monteleone et al., 2017). Inhibition of miRNA-708 causes increased activity of EYA3: this causes genomic instability which leads to uninterrupted tumor cell growth and continuous repair of replicative and oxidative stress induced DNA damage in order to deter proliferation arrest. Moreover, it also makes tumor cells chemo resistant, aggressive, and stimulate angiogenesis and the development of metastasis like properties in EWS cells. Deleting or inhibiting the EYA3 activates an array of protein cascades which suppress tumor cell proliferation, induce apoptosis, stabilize genomic expression and stimulate angiogenesis as evident from Wang et al., (2021) study. In their study, benzarone (BZ) was used to evaluate the inhibitory effect on EYA3. It was observed that BZ impaired the tumor proliferation in A673 cells in a dose dependent manner and reduced the expression of EYA3, which in turn regulated the angiogenic and VEGF-A function. Unfortunately, BZ induces severe hepatotoxicity and can cause other life-threatening side effects. Therefore, in our study we adopted the safer insilico approach which uses medicinal compounds to target EYA3 to obtain good cytotoxic inhibitor for EWS.

More than 2,000 medicinal compounds participated in the screening analysis to obtain possible inhibitors showing interaction with the EYA3 protein. All these compounds had adequate ADMET and druglikeness qualities to avert any mishap during clinical trials and in vitro experiments. Virtual screening revealed two compounds (Sorbifolin and 1,7-dihydroxy-3-

methylanthracene-9.10-dione), which can interact with the active residues via hydrogen bonding. Both compounds exploited terminal hydroxyl groups to establish hydrogen bonds, whereas benzene rings formed hydrophobic pi-anionic bonds. The intermolecular interaction energy was adequate and the RMSD comparison with benzarone was ≈ 2.24-2.63 Å, within the range of stability (Shah et al., 2020, 2021).

These compounds were also subjected to toxicity analysis. This showed that a high toxic dose level is required to initiate a deleterious response which is confined to the liver, heart, urinary bladder, pituitary gland, kidney, and stomach. These responses can effectively be dealt by using nanotechnological delivery methods to avert the side effects and further improve the effectiveness of the compounds (Patra et al., 2018). PASS and gene expression studies revealed some important findings: both compounds are HIF1-alpha (Hypoxia inducible factor alpha) inhibitors. HIF1-alpha is implicated in mediating tumor cell evasion by inhibiting apoptotic factors, and immunological influence (El-Naggar et al., 2015) and also provide chemotherapy resistance. The compounds are also anti-neoplastic agents. They enhance TP53 expression (Thoenen et al., 2019): when this is upregulated, tumor suppression in this disease is averted.

Sorbifolin has a downregulatory effect on the E2F5 transcription factor that drives the continuous cell cycle in EWS cells (Schwentner et al., 2015) and also on the STEAP1 (Grunewald et al., 2012) gene. This stimulates the formation of invasive phenotypes and provides tumor cells with migratory properties resulting in metastasis. This compound also activates the expression of NOTCH1, which helps to induce apoptosis, in these tumor cells (Di Muccio et al., 2005). 1,7-dihydroxy-3-methylanthracene-9.10-dione also exhibited a downregulatory effect on CTSD gene, helping EWS cells to metastasize.

Another step was also incorporated into our study, predicting the cytotoxic effects of these compounds on the A673 EWS cell line using the PaccMann database. Results showed that Sorbifolin had a better IC_{50} value than 1,7-dihydroxy-3-methylanthracene-9.10-dione, providing further evidence to our screening studies as Sorbifolin established more interactions as compared to the other compound.

In conclusion, to the best of our knowledge, we are the first to report two medicinal compounds as lead candidates for the EYA3 drug target of Ewing Sarcoma. These compounds showed desirable affinity with the EYA3 protein: they have safe toxicity attributes and possess potential side effects which can be dealt with using nanotechnology and pharmacokinetic calibration. In silico PASS and gene expression profiles of these compounds further explained the therapeutic mechanism. Cell lining studies showed that Sorbifolin has a higher IC50 value and cytotoxic activity than 1,7-dihydroxy-3-methylanthracene-9.10-dione. Our study provided a 3D constructed EYA3 model and two promising medicinal compounds showing affinity for this protein. The results of these studies are under in vitro analysis to further corroborate our in-silico findings.

Author Contribution Statement

All authors contributed equally in this study.

Acknowledgements

References

Ahmed AA, Zia H, Wagner L (2014). Therapy resistance mechanisms in Ewing's sarcoma family tumors. *Cancer Chemother Pharmacol*, **73**, 657–63.

Bellan DG, Filho RJG, et al (2015). Ewing's Sarcoma: Epidemiology And Prognosis For Patients Treated At The Pediatric Oncology Institute, Iop-Graacc-Unifesp. *Rev Bras Ortop*, **47**, 446–50.

Cadow J, Born J, Manica M, et al (2020). PaccMann: a web service for interpretable anticancer compound sensitivity prediction. *Nucleic Acids Res*, **48**, 502-8.

Campbell K, Shulman D, Janeway KA, et al (2018). Comparison of Epidemiology, Clinical Features, and Outcomes of Patients with Reported Ewing Sarcoma and PNET over 40 Years Justifies Current WHO Classification and Treatment Approaches. *Sarcoma*, **2018**, 1712964.

Di Muccio T, Baliko F, Alman BA (2005). Notch-1 signaling in Ewing's sarcoma. *Cancer Res*, **65**, 67 LP – 67.

El-Naggar AM, Veinotte CJ, Cheng H, et al (2015). Translational Activation of HIF1α by YB-1 Promotes Sarcoma Metastasis. *Cancer Cell*, **27**, 682–97.

Gemoll T, Epping F, Heinrich L, et al (2015). Increased cathepsin D protein expression is a biomarker for osteosarcomas, pulmonary metastases and other bone malignancies. *Oncotarget*, **6**, 16517–26.

Grunewald TGP, Diebold I, et al (2012). STEAP1 Is Associated with the Invasive and Oxidative Stress Phenotype of Ewing Tumors. *Mol Cancer Res*, **10**, 52 LP – 65.

Grünewald TGP, Cidre-Aranaz F, et al (2018). Ewing sarcoma. *Nat Rev Dis Prim*, **4**, 1–22.

Heo L, Park H, Seok C (2013). GalaxyRefine: Protein structure refinement driven by side-chain repacking. *Nucleic Acids Res*, **41**, 384–8.

Ivanov SM, Lagunin AA, et al (2018). ADVERPred–Web service for prediction of adverse effects of drugs. *J Chem Inf Model*, **58**, 8–11.

Jendele L, Krivak R. et al (2019). PrankWeb: a web server for ligand binding site prediction and visualization. N*ucleic Acids Res*, **47**, 345–9.

Kabir W, Choong PFM (2021). The Epidemiology and Pathogenesis of Sarcoma. Sarcoma. Springer, pp 11–27.

Kopp J, Schwede T (2004). The SWISS-MODEL Repository of annotated three-dimensional protein structure homology models. *Nucleic Acids Res*, **32**, 230–4.

Lagunin, A Zakharov, et al (2011). QSAR modelling of rat acute toxicity on the basis of PASS prediction. *Mol Inform*, **30**, 241–50.

Lagunin A, Ivanov S, et al (2013). DIGEP-Pred: web service for in silico prediction of drug-induced gene expression profiles based on structural formula. *Bioinformatics*, **29**, 2062–3.

Lagunin A, Rudik A, et al (2018). ROSC-Pred: web-service

for rodent organ-specific carcinogenicity prediction. *Bioinformatics*, **34**, 710–2.

Lupo PJ, Spector LG, et al (2021). Epidemiology of Bone and Soft Tissue Sarcomas. Sarcomas Bone Soft Tissues Child Adolesc Springer, pp 1–16.

May WA, Grigoryan RS, et al (2013). Characterization and Drug Resistance Patterns of Ewing's Sarcoma Family Tumor Cell Lines. *PLoS One*, **8**, e80060.

Monteleone NJ, Lutz CS (2017). miR-708-5p: a microRNA with emerging roles in cancer. *Oncotarget*, **8**, 71292–316.

Patra JK, Das G, et al (2018). Nano based drug delivery systems: recent developments and future prospects. *J Nanobiotechnol*, **16**, 71.

Pilon AC, Valli M, et al (2017). NuBBEDB: an updated database to uncover chemical and biological information from Brazilian biodiversity. *Sci Rep*, **7**, 7215.

Poroikov VV, Filimonov DA, et al (2003). PASS Biological Activity Spectrum Predictions in the Enhanced Open NCI Database Browser. *J Chem Inf Comput Sci*, **43**, 228–36.

Robin TP, Smith A, et al (2012). EWS/FLI1 Regulates EYA3 in Ewing Sarcoma via Modulation of miRNA-708, Resulting in Increased Cell Survival and Chemoresistance. *Mol Cancer Res*, **10**, 1098 LP – 1108.

Schwentner R, Papamarkou T, et al (2015). EWS-FLI1 employs an E2F switch to drive target gene expression. *Nucleic Acids Res*, **43**, 2780–9.

Shah FH, Salman S, et al (2020). In silico study of thymohydroquinone interaction with blood–brain barrier disrupting proteins. *Futur Sci OA*, FSO632.

Shah FH, Kim SJ (2021). Targeting FGL2, a molecular drug target for glioblastoma, with natural compounds through virtual screening method. *Future Med Chem*, **13**, 805–16.

Thoenen E, Curl A, Iwakuma T (2019). TP53 in bone and soft tissue sarcomas. *Pharmacol Ther*, **202**, 149–64.

Velázquez-Libera JL, Durán-Verdugo F, et al (2020). LigRMSD: a web server for automatic structure matching and RMSD calculations among identical and similar compounds in protein-ligand docking. *Bioinformatics*, **36**, 2912–4.

Wang Y, Pandey RN, Roychoudhury K, et al (2021). Targeting EYA3 in Ewing Sarcoma Retards Tumor Growth and Angiogenesis. *Mol Cancer Ther*, **20**, 803 – 15.